LAWRENCE
LIVERMORE
NATIONAL
LABORATORY

LLNL-CONF-471992

High Temperature Chemical Kinetic Combustion Modeling of Lightly Methylated Alkanes

S. M. Sarathy, C. K. Westbrook, W. J. Pitz, M. Mehl

March 4, 2011

European Combustion Meeting 2011
Cardiff, United Kingdom
June 27, 2011 through July 1, 2011

Disclaimer

High Temperature Chemical Kinetic Combustion Modeling of Lightly Methylated Alkanes

S. Mani Sarathy[1*], Charles K. Westbrook[1], William J. Pitz[1], and Marco Mehl[1]

[1] *Physical and Life Sciences Directorate, Lawrence Livermore National Laboratory, 7000 East Avenue, Livermore, CA 94551, USA*

Abstract

Conventional petroleum jet and diesel fuels, as well as alternative Fischer-Tropsch (FT) fuels and hydrotreated renewable jet (HRJ) fuels, contain high molecular weight lightly branched alkanes (i.e., methylalkanes) and straight chain alkanes (n-alkanes). Improving the combustion of these fuels in practical applications requires a fundamental understanding of large hydrocarbon combustion chemistry. This research project presents a detailed high temperature chemical kinetic mechanism for *n*-octane and three lightly branched isomers octane (i.e., *2*-methylheptane, *3*-methylheptane, and *2,5*-dimethylhexane). The model is validated against experimental data from a variety of fundamental combustion devices. This new model is used to show how the location and number of methyl branches affects fuel reactivity including laminar flame speed and species formation.

Introduction

Detailed chemical kinetic combustion models of real fuels (e.g., gasoline, diesel, and jet fuels) are important tools for improving the design, efficiency, and environmental performance of combustion technologies. Fuels derived from conventional petroleum feedstock often are comprised of thousands of different hydrocarbon compounds. This complexity makes it challenging to develop detailed chemical kinetic models of real fuels because modeling each fuel component would be computationally expensive. One way of reducing complexity is to group fuel compounds together into structural classes, and formulate a smaller "surrogate fuel" model that represents the chemical and physical characteristics of the real fuel. In this way the chemical kinetic model becomes easier to build and less computationally expensive to solve in a reacting flow simulation.

Previous studies at the Lawrence Livermore National Laboratory have presented detailed chemical kinetic models for several important structural classes found in real fuels, such as *n*-alkanes [1,2], *iso*-alkanes [3,4,5,6], alkenes [7,8], aromatics [10], and cyclo-alkanes [11,12]. Surrogate fuel models have also been developed for gasoline fuel [10,13] and gasoline and diesel primary reference fuels [14] by merging the models of relevant structural classes. A recent review paper by Pitz and Mueller [15] describes the development of diesel surrogate fuel models. The composition of typical diesel fuels is presented as a mixture of high molecular weight (i.e., C_{10}-C_{20}) *n*-alkanes, lightly branched *iso*-alkanes with one or two methyl groups, cycloalkanes with multiple alkyl side chains, and aromatics with multiple side chains. The recent progress in combustion modeling of these structural classes is discussed in detail; however, the authors conclude that major research gaps remain in modeling high molecular weight (i.e., greater than C_{10}) aromatics, alkyl aromatics, cyclo-alkanes, and lightly branched *iso*-alkanes.

The focus of the present research study is on high molecular weight *3*-methylheptane, *2*-methylheptane, *2,5*-dimethylhexane, and *n*-octane. These structures are important components of conventional diesel fuels derived from petroleum, synthetic Fischer-Tropsch diesel and jet fuels derived coal, natural gas, and/or biomass, and renewable diesel and jet fuels derived from thermochemical treatment of bio-derived fats and oils (e.g., hydrotreated renewable jet (HRJ) fuels). Significant effort is placed on understanding the effect methyl substitution on important combustion properties.

Chemical Kinetic Mechanism Formulation

The proposed detailed chemical kinetic mechanism includes high-temperature kinetic schemes for *2*-methylheptane, *3*-methylheptane, and *2,5*-dimethylhexane. We include the important reaction pathways based on the early work of Curran et al. on *n*-heptane and *iso*-octane [1,3]. In addition, we include an updated version of our *n*-octane sub-mechanism initially developed by Westbrook et al. [2]. The "core mechanism" used here is our latest detailed mechanism for *n*-heptane, which was presented and discussed as part of the gasoline surrogates model by Mehl et al. [10,13]. This core mechanism is comprised of an updated C_0-C_5 sub-mechanism [16,17], the C_6-C_7 alkane sub-mechanism from Mehl et al. [10,13], and the C_5-C_7 alkenes sub-mechanism from Mehl et al. [7,8].

Naming of Species

To illustrate the naming of the species for the 2-methylalkanes mechanism, 2-methylheptane is denoted as C8H18-2 in the mechanism, for example (see Figure 1 for its molecular structure). The carbon chain is labeled numerically (i.e., 1, 2, 3, etc.) such that the location number of the methyl branch is minimized. For 2-methylheptene species, the location of a double bond is identified by a hyphen followed by the number of the first carbon in the double bond (e.g., 2-methyl-3-heptene is C7H14-3-2). Additional notations are provided to denote

radical sites in the molecule. The carbon sites are labeled alphabetically (i.e., a, b, c, etc.) such that the location of the first methyl branch is minimized (Figure 1). In this way, the 2-methyl-3-heptyl radical is denoted as C7H15-2c, while the 2-methyl-1-heptyl radical is written as C7H15-2a.

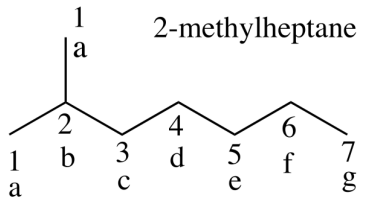

Figure 1 - Structure of 2-methylheptane (C_8H_{18}-2)

Classes of Reactions

The major classes of elementary reactions considered for the oxidation of octane isomers include the following:

High Temperature Reaction Classes

1. Unimolecular fuel decomposition
2. H-atom abstraction from the fuel
3. Alkyl radical decomposition
4. Alkyl radical isomerization
5. H-atom abstraction reactions from alkenes
6. Addition of radical species O and OH to alkenes
7. Alkenyl radical decomposition
8. Alkene decomposition

Thermochemical Data

The thermodynamic parameters for the species are very important because they are used to determine reverse rate constants. The THERM [20] software was used to compute the thermochemical properties of species not present in the *n*-alkane model [2]. The THERM group values are from Benson [21] and Bozzelli [22,23].

Tranport Properties

Kinetic processes and transport processes are rate controlling in diffusion flames and droplet vaporization/combustion, so transport properties are needed for all the species in the model. This study obtained the molecular transport parameters for species using a variety of methods. The transport properties for species upto C_8 were already available in a previously published *2*-methylheptane model [18,19]. The transport properties of larger alkanes, alkene, alkyl, and alkenyl species were determined as follows. For stable species, this study used the correlations developed by Tee, Gotoh, and Stewart [24], as described in Holley and coworkers for hydrocarbons [25], to calculate the LJ collision diameter and potential well depth using the critical pressure (Pc), critical temperature (Tc), and boiling point (Tb) of the species. Pc, Tc, and Tb for the majority stable species are based on the recommendations of Owczarek and Blazej [26,27], and the data for missing species was extrapolated. Following previous work [28], the polarizability in cubic Angstroms of stable species was calculated using an empirical correlation [29], which depends on the number of C, H, and O atoms in the molecule. The values calculated using this method were comparable to experimentally measured polarizability for species where such data was available [30]. The dipole moment for all new species was set to zero because they are non-polar hydrocarbons [31]. The index factor, which describes the geometry of the molecule was determined from the molecular structure (i.e., 0 for atoms, 1 for linear molecules, and 2 for nonlinear molecules.

Validation Studies

In recent studies, the proposed model for *n*-octane and *2*-methylheptane was validated against a wide range of experimental data from RCMs, JSR, shock tube, premixed laminar flames, and counterflow non-premixed flames [18,19]. Westbrook et al. [2] previously validated the C_8-C_{16} *n*-alkane mechanism; the present improvements to the reaction classes and rate rules do not significantly alter the validations presented previously. In this study, we include present several validations for *n*-octane and *2*-methylheptane since these are the only molecules for which data was readily available. Validating the mechanism against *2*-methylheptane is considered adequate because the same reaction rate rules are applied for *3*-methylheptane and *2,5*-dimethylhexane.

Laminar Flame Speed Experiments and Simulations of *n*-octane and *2*-methylheptane

Laminar flame speed, S_u^0, experiments were carried out in the counterflow configuration at atmospheric pressure and an unburned reactant temperature of 353 K and presented previously [19,32]. Figure 2 depicts both experimental data and numerical predictions for the S_u^0's of *2*-methylheptane/air and *n*-octane/air flames; the experimental data for *n*-octane/air flames were taken from [32]. S_u^0 of 2-methylheptane/air flames are consistently 3.5-5 cm/s lower than those of *n*-octane/air flames. This is expected, as it has previously established that branching in the fuel molecular structure reduces reactivity and as a result S_u^0. The current model reproduces successfully the relative reactivities of these two fuels. The peak for both *n*-octane/air and 2-methylheptane/air flames occurs at $\phi \approx 1.05$. The predictions of the current model are in good agreement with the experimental data for 2-methylheptane flames for $0.70 \leq \phi \leq 1.10$. At higher ϕ's, the model is over predicting the experimental results by approximately 4 cm/s. For *n*-octane/air flames, the trends between the model and the experimental data taken from [32] are similar,

i.e., there is good agreement for lean to stoichiometric conditions, and the model consistently over predicts the experimental results for fuel rich conditions. Figure 3 presents n-octane/air premixed laminar flame velocities at range of pressures [54] as an additional validation target for the proposed mechanism. The model exhibits excellent agreement with the experimental data at 1 atm and 2 atm. At 5 atm, the model under predicts the laminar flame velocity at equivalence rations greater than 0.9.

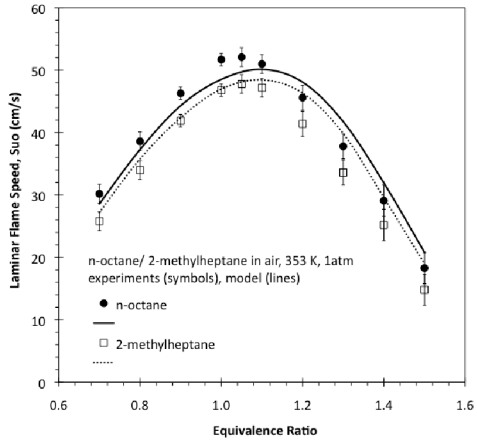

Figure 2 – Laminar flame speeds of *n*-octane (Ji et al [32]) and 2-methylheptane in air at 353 K and 1 atm.

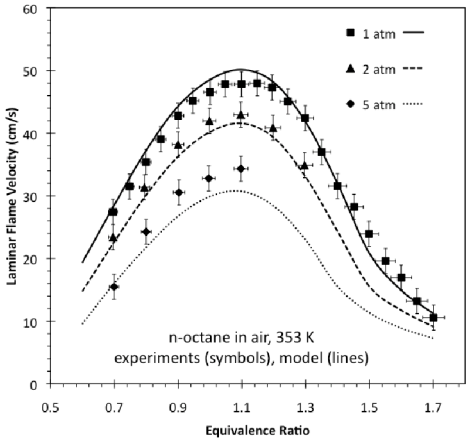

Figure 3 – Laminar flame speeds of *n*-octane (Kelley et al. [33]) at 353 K and various pressures.

Laminar Flame Speed Simulations of octane isomers

Simulated laminar flame speeds for the octane isomers are shown in Figure 4. The proposed model predicts that the laminar flame speed reduces as the number of methyl branches increases. For example, *2,5*-dimethylhexane has laminar flame speeds approximately 1.5-3.0 cm/s slower than *2*-methylheptane.

In order to elucidate the reasons for lower flame speeds in branched alkanes, a reaction flux analysis was conducted for at stoichiometric conditions and a temperature of approximately 1000 K. The results show that H-atom abstraction from the tertiary C-H site in *2*-methylheptane and *2,4*-dimethylhexane is followed by β-scission leading to the formation of *iso*-butene and subsequently the resonantly stabilized *iso*-butenyl radical. An analogous reaction sequence in *n*-octane leads to *1*-butene and subsequently the *1*-butenyl radical. The increased stability of the *iso*-butenyl radical compared to the *1*-butenyl is the reason for lower flame speeds in the branched alkanes. The flame speed for *2,5*-dimethylhexane is lower than that of *2*-methylheptane because there are two tertiary C-H sites which increase the production of *iso*-butene.

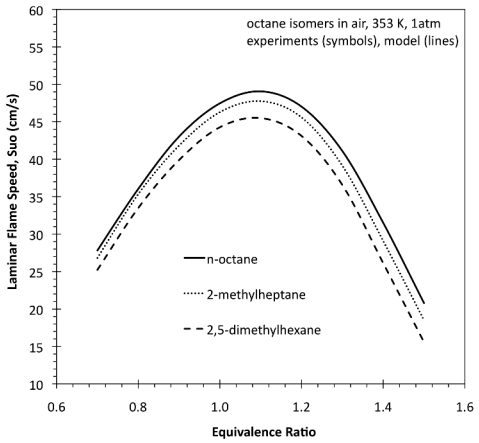

Figure 4 – Laminar flame speeds of octane isomers at 353 K and 1 atm.

Conclusions

This study presented a high temperature oxidation mechanism for four octane isomers. Premixed laminar flame speeds are slower for 2-methylheptane when compared to *n*-octane because of the increased production of the resonantly stabilized *iso*-butenyl radical. Model predictions indicate that *2,5*-dimethylhexane has an even lower flame speed due to the increased number of tertiary C-H sites.

The proposed chemical kinetic mechanism has the potential of significantly improving our understanding diesel and jet fuel combustion. The

structures present within the mechanism can be used to develop surrogate fuel formulations for a wide variety of fuels, such as conventional petroleum derived fuels, synthetic Fischer-Tropsch fuels, and renewable fuels derived from thermochemical treatment of bio-derived fats and oils (e.g., HRJ fuels). Therefore, the present study provides immediate potential of improving the chemical fidelity of surrogate fuel models. We plan to extend the proposed model to include low temperature reaction pathways and oxidation chemistry for larger hydrocarbons upto C_{20}.

Acknowledgments

This work was supported by the US Department of Energy, Office of Vehicle Technologies and the Office of Basic Energy Sciences, and the authors thank program managers Gurpreet Singh, Kevin Stork, and Wade Sisk. This work was performed under the auspices of the US Department of Energy by Lawrence Livermore National Laboratory under Contract DE-AC52-07NA27344.

7. References

1. H.J. Curran, P. Gaffuri, W.J. Pitz, C.K. Westbrook, Combust. Flame 114 (1998) 149-177.
2. C.K. Westbrook, W.J. Pitz, O. Herbinet, H.J. Curran, E.J. Silke, Combust. Flame 156 (2009) 181-199.
3. H.J. Curran, P. Gaffuri, W.J. Pitz, C.K. Westbrook, Combust. Flame 129 (2002) 253-280.
4. M.A. Oehlschlaeger, J. Steinberg, C.K. Westbrook, W.J. Pitz, Combust. Flame 156 (2009) 2165-2172.
5. C.K. Westbrook, W.J. Pitz, J.E. Boercker, H.J. Curran, J.F. Griffiths, C. Mohamed, M. Ribacour, Proc. Combust. Inst. 29 (2002) 1311-1318.
6. C.K. Westbrook, W.J. Pitz, H.J. Curran, J. Boercker, E. Kunrath, Int. J. Chem. Kinet. 33 (12) (2001) 868-877.
7. M. Mehl, G. Vanhove, W.J. Pitz, E. Ranzi. Combust. Flame 155 (4) (2008) 756-772.
8. M. Mehl, W.J. Pitz, C.K. Westbrook, K. Yasunaga, C. Conroy, H.J. Proc. Combust. Inst. 33
9. (2011) 201-208.
10. M. Mehl, W.J. Pitz , C.K. Westbrook, H.J. Curran, Proc. Combust. Inst. 33 (2011) 193-200.
11. E.J. Silke, W.J. Pitz, C.K. Westbrook, J. Phys. Chem. A 111 (2007) 3761-3775.
12. W.J. Pitz, C.V. Naik, T.N. Mhaolduin, C.K. Westbrook, H.J. Curran, J.P. Orme, J.M. Simmie, Proc. Combust. Inst. 31 (2007) 267-275,
13. M. Mehl, W. J. Pitz, M. Sjöberg, J. E. Dec, SAE 2009 International Powertrains, Fuels and Lubricants Meeting, SAE Paper No. 2009-01-1806, Florence, Italy.
14. C.K. Westbrook, W.J. Pitz, M. Mehl, H.J. Curran, Proc. Combust. Inst. 33 (2011) 185-192.
15. W.J. Pitz, C.J. Mueller, Prog. Energy Comb. Sci. (2010), doi:10.1016/j.pecs.2010.06.004.
16. M.V. Johnson, S.S. Goldsborough, Z. Serinyel, et al., Energy Fuels 23 (2009) 5886–5898.
17. J. Moc, G. Black, J.M. Simmie, H.J. Curran, AIP Conf. Proc. 1148 (2009) 161–164.
18. S.M. Sarathy, C. Yeung, C.K. Westbrook, W.J. Pitz, M. Mehl, M.J. Thomson. Combust. Flame. (2010) dx.doi.org/10.1016/j.combustflame.2010.11.00
19. S.M. Sarathy, C.K. Westbrook, W.J. Pitz, M. Mehl, C. Togbe, P.Dagaut, H. Wang, M.A. Oehlschlaeger, U. Niemann, K. Seshadri, U. Niemann, P.S. Veloo, C. Ji, F. Egolfopoulos, T. Lu. Submitted to Combust. Flame. (March 2011)
20. E.R. Ritter, J.W. Bozelli, Int. J. Chem. Kin. 23 (1991) 767-778.
21. S.W. Benson, Thermochemical Kinetics (2nd ed.), Wiley, New York (1976).
22. T.H. Lay, J.W. Bozzelli, A.M. Dean, E.R. Ritter, J. Phys. Chem. 99 (1995) 14514-14527.
23. Bozzelli, J. W. Personal communication, new THERM version, 2003.
24. L.S. Tee, S. Gotoh, W.E. Stewart, Ind. Eng. Chem. Fundam. 5 (3) (1966) 356-363.
25. A.T. Holley, Y. Dong, M.G. Andac, F.N. Egolfopoulos, Combust. Flame 144 (2006) 448-460.
26. I. Owczarek, K. Blazej, J. Phys. Chem. Ref. Data, 32 (4) (2003) 1411-1427.
27. I. Owczarek, K. Blazej, J. Phys. Chem. Ref. Data, 35 (4) (2006) 1461-1474.
28. S.M. Sarathy, M.J. Thomson, W.J. Pitz, T. Lu, Proc. Combust. Inst. 33 (2011) 399-405.
29. R. Bosque, J. Sales, J. Chem. Inf. Comp. Sci. 42 (2002) 1154-1163.
30. D. R. Lide (Ed.), CRC Handbook of Chemistry and Physics, 87th Edition, Taylor and Francis, Boca Raton, FL, 2007.
31. A.L. McClellan, Tables of Experimental Dipole Moments, Freeman, San Francisco, 1963.
32. C. Ji, E. Dames, Y.L. Wang, H. Wang, F.N Egolfopoulos, Combust. Flame 157 (2010) 277–287.
33. A. Kelley, W. Liu, Y. Xin, A. Smallbone, and C. Law, *Proc. Combust. Inst.,* 33 (2010), 501-508.
34. T.F. Lu, and C.K. Law, *Proc. Combust. Inst.,* 30 (2005), 1333-1341.

35. Z. Luo, T. Lu, M. Maciaszek, S. Som, and D. Longman, *Energy Fuels,* 24 (2010), 6283–6293.
36. T.F. Lu, and C.K. Law, *Combust. Flame,* 144 (2006), 24-36.
37. A.E. Lutz, R.J. Kee, and J.A. Miller, *Technical Report SAND87-8248, Sandia National Laboratories* (1987).
38. P. Glarborg, R. Kee, J. Grcar, and J. Miller, *SAND86-8209, Sandia National Laboratories* (1986).
39. T.F. Lu, and C.K. Law, *Prog. Energy Combust. Sci.,* 35 (2009), 192-215.
40. K. Seshadri, T.F. Lu, O. Herbinet, S.B. Humer, U. Niemann, W.J. Pitz, R. Seiser, and C.K. Law, *Proc. Combust. Inst.,* 32 (2009), 1067-1074.
41. X.L. Zheng, T.F. Lu, and C.K. Law, *Proc. Combust. Inst.,* 31 (2007), 367-375.
42. R. Sankaran, E.R. Hawkes, J.H. Chen, T.F. Lu, and C.K. Law, *Proc. Combust. Inst.,* 31 (2007), 1291-1298.
43. V. Giovangigli and M. D. Smooke, *Combust. Sci. Technol.* 53 (1) (1987) 23-49.
44. M. Nishioka, C. K. Law and T. Takeno, *Combust. Flame* 104 (3) (1996) 328-342.
45. K. Seshadri, F. Williams, *Int. J. Heat Mass Trans.* 21 (1978) 251-253.